New Phytologist

Research

Rhizosheath drought responsiveness is variety-specific and a key component of belowground plant adaptation

Franziska A. Steiner[1], Andreas J. Wild[2], Nicolas Tyborski[3], Shu-Yin Tung[1,4], Tina Koehler[5], Franz Buegger[6], Andrea Carminati[7], Barbara Eder[8], Jennifer Groth[8], Benjamin D. Hesse[9,10], Johanna Pausch[2], Tillmann Lüders[3], Wouter K. Vahl[8], Sebastian Wolfrum[4], Carsten W. Mueller[11,12] and Alix Vidal[13]

[1]Soil Science, TUM School of Life Sciences, Technical University of Munich, 85354, Freising, Germany; [2]Agroecology, Bayreuth Center of Ecology and Environmental Research (BayCEER), University of Bayreuth, 95447, Bayreuth, Germany; [3]Ecological Microbiology, Bayreuth Center of Ecology and Environmental Research (BayCEER), University of Bayreuth, 95448, Bayreuth, Germany; [4]Institute for Agroecology and Organic Farming, Bavarian State Research Center for Agriculture, 85354, Freising, Germany; [5]Root-Soil Interaction, TUM School of Life Sciences, Technical University of Munich, 85354, Freising, Germany; [6]Research Unit Environmental Simulation, Helmholtz Zentrum München (GmbH), German Research Center for Environmental Health, 85764, Neuherberg, Germany; [7]Physics of Soils and Terrestrial Ecosystems, Department of Environmental Systems Science, ETH Zurich, 8092, Zurich, Switzerland; [8]Institute for Crop Science and Plant Breeding, Bavarian State Research Center for Agriculture, 85354, Freising, Germany; [9]Chair of Land Surface-Atmosphere Interactions, TUM School of Life Sciences, Technical University of Munich, 85354, Freising, Germany; [10]Department of Integrative Biology and Biodiversity Research, Institute of Botany, University of Natural Resources and Life Sciences, 1180, Vienna, Austria; [11]Chair of Soil Science, Institute of Ecology, Technische Universität Berlin, 10587, Berlin, Germany; [12]Department for Geoscience and Natural Resource Management, University of Copenhagen, 1350, Copenhagen, Denmark; [13]Soil Biology Group, Department of Environmental Sciences, Wageningen University, 6700, Wageningen, the Netherlands

Author for correspondence:
Franziska A. Steiner
Email: f.steiner@tum.de

Received: *30 September 2023*
Accepted: *2 February 2024*

New Phytologist (2024) **242:** 479–492
doi: 10.1111/nph.19638

Key words: crop, maize, rhizodeposition, rhizosphere, soil aggregation, soil organic carbon, soil structure, water scarcity.

Summary

- Biophysicochemical rhizosheath properties play a vital role in plant drought adaptation. However, their integration into the framework of plant drought response is hampered by incomplete mechanistic understanding of their drought responsiveness and unknown linkage to intraspecific plant–soil drought reactions.
- Thirty-eight *Zea mays* varieties were grown under well-watered and drought conditions to assess the drought responsiveness of rhizosheath properties, such as soil aggregation, rhizosheath mass, net-rhizodeposition, and soil organic carbon distribution. Additionally, explanatory traits, including functional plant trait adaptations and changes in soil enzyme activities, were measured.
- Drought restricted soil structure formation in the rhizosheath and shifted plant–carbon from litter-derived organic matter in macroaggregates to microbially processed compounds in microaggregates. Variety-specific functional trait modifications determined variations in rhizosheath drought responsiveness. Drought responses of the plant–soil system ranged among varieties from maintaining plant–microbial interactions in the rhizosheath through accumulation of rhizodeposits, to preserving rhizosheath soil structure while increasing soil exploration through enhanced root elongation.
- Drought-induced alterations at the root–soil interface may hold crucial implications for ecosystem resilience in a changing climate. Our findings highlight that rhizosheath soil properties are an intrinsic component of plant drought response, emphasizing the need for a holistic concept of plant–soil systems in future research on plant drought adaptation.

Introduction

In the coming decades, the frequency and severity of drought events is predicted to increase (Spinoni *et al.*, 2018; Intergovernmental Panel on Climate Change, 2023), which will significantly diminish global crop yields (Leng & Hall, 2019; Santini *et al.*, 2022). Consequently, great research efforts have focused on identifying phenotypic properties, that is functional traits, that promote the drought tolerance of plants, such as beneficial morphological and physiological root traits (Comas *et al.*, 2013; Klein *et al.*, 2020; Lynch *et al.*, 2021). However, accumulating evidence suggests that biological and physicochemical interactions at the root–soil interface further facilitate plant drought tolerance (Rabbi *et al.*, 2021, 2022; Aslam *et al.*, 2022; Cheraghi *et al.*, 2023). In this context, the rhizosheath, defined as the soil adhering to the root after excavation (George *et al.*, 2014; Pang *et al.*, 2017), receives increasing attention as it preserves root–soil contact and consequently nutrient and water uptake during soil

desiccation (North & Nobel, 1997; George *et al.*, 2014; Pang *et al.*, 2017; Cheraghi *et al.*, 2023). Furthermore, the rhizosheath is the most biologically active compartment within the rhizosphere, which encompasses the entire soil volume influenced by roots (Ndour *et al.*, 2020). Recent studies by Rabbi *et al.* (2021) and Rabbi *et al.* (2022) emphasized the importance of rhizosheath properties in determining intraspecific variation in plant drought tolerance, highlighting the potential of integrating rhizosheath properties as important phenotypic traits in the framework of plant drought adaptation.

While root-engineered rhizosheath properties are increasingly recognized as inherent phenotypic plant traits (Adu *et al.*, 2017; De La Fuente Cantó *et al.*, 2020), the assessment of their importance for plant drought adaptation is hampered by the lack of studies investigating drought-induced modifications of biophysicochemical rhizosheath properties, such as changes in physical structure or biogeochemical cycles. We propose, for example, that drought alters the formation of soil aggregates, soil units composed of mineral particles, organic, and biotic materials (Tisdall & Oades, 1982; Totsche *et al.*, 2018), within the crop rhizosheath. This is supported by Alami *et al.* (2000), who reported an increase in macroporosity in the rhizosheath of drought-stressed sunflowers. Additionally, various biotic and abiotic drivers of soil aggregation have been suggested to change with soil desiccation. For instance, a reduction in soil moisture can directly alter aggregate formation by enhancing interparticle contacts through contraction of water menisci (Horn & Dexter, 1989; Carminati *et al.*, 2008). Also, altered inputs of root-derived carbon (C) are likely to feedback on soil aggregation through the changed supply of organic gluing agents (Tisdall & Oades, 1982; Morel *et al.*, 1991; Baumert *et al.*, 2018). However, labile C inputs into the soil via rhizodeposition (i.e. root exudates, root border cells, and mucilage, Jones *et al.* (2009)) have been described to vary in response to drought from increased (Somasundaram *et al.*, 2009; Ulrich *et al.*, 2022) to decreased amounts (Bakhshandeh *et al.*, 2018; De Vries *et al.*, 2019; Wang *et al.*, 2021; Zhang *et al.*, 2023). These changes in plant-C inputs can potentially mediate drought effects on the root-surrounding soil microbiome, yet findings across studies are conflicting. Several studies highlight that preserved rhizodeposition mitigates drought effects on the microbial community and microbial-driven soil nutrient cycling (Ahmed *et al.*, 2018; De Vries *et al.*, 2019; Zhang *et al.*, 2021). Other studies suggest that drought stress decouples preserved rhizodeposition and microbial plant-C utilization and enzyme activity (Karlowsky *et al.*, 2018; Zhang *et al.*, 2023). Consequently, drought-induced changes in the balance between direct accumulation of plant-derived C and its incorporation after microbial processing can significantly impact the retention of soil organic C (Kallenbach *et al.*, 2016; Angst *et al.*, 2021) and its distribution among aggregate fractions of different sizes and life spans (Verchot *et al.*, 2011; Angst *et al.*, 2021). In summary, previous work has demonstrated that water scarcity can greatly alter biophysicochemical rhizosheath properties and the intricate functional relationships between soil, microbial, and plant traits. Yet, the large variability between studies underscores the limited systemic understanding of the drought responsiveness of rhizosheath traits.

When studying plasticity, or an organism's adaptation to a changing environment, it is crucial to consider the entire phenotype rather than isolated trait responses, as changes in their expression are closely interlinked (Blum, 1996; Forsman, 2015; Schneider, 2022). Particularly under drought, the reduced photosynthetic activity (e.g. Ulrich *et al.*, 2022; Werner *et al.*, 2022) reinforces the trade-off for the plant to partition recent photoassimilates efficiently between traits for soil resource acquisition, such as rhizodeposition, microbial symbiosis, and root growth (Palta & Gregory, 1997; Bakhshandeh *et al.*, 2018; Karlowsky *et al.*, 2018; Wang *et al.*, 2021). The prioritization of certain functional traits under drought stress likely links these adaptation strategies mechanistically to the modification of specific soil properties. For instance, modifications in root morphology and physiology to cope with water scarcity (De Vries *et al.*, 2016; Bakhshandeh *et al.*, 2018; Karlowsky *et al.*, 2018; Klein *et al.*, 2020) have direct implications for the rhizosheath, such as changes in root elongation determining longitudinal rhizosheath elongation (Holz *et al.*, 2018). Yet, the drought responsiveness of key functional traits can be highly variable within plant species (Adu *et al.*, 2017; Bakhshandeh *et al.*, 2018; Klein *et al.*, 2020; Naylor *et al.*, 2023), suggesting that the corresponding drought reaction of the plant–soil system is likewise driven by significant intraspecific variability. Thus, it is crucial to understand the drought responsiveness of rhizosheath properties in interaction with variety-specific drought responses of the entire plant–soil system.

In a phenotyping experiment with 38 maize varieties grown under well-watered and drought conditions, we characterized the drought responsiveness of physicochemical rhizosheath properties, namely soil aggregation, net rhizodeposition, and the distribution of soil organic carbon (SOC) and rhizodeposit-C across aggregate fractions. In addition, we assessed the mechanistic link between rhizosheath drought responses and drought modifications of specific functional plant traits to improve the understanding of drought reactions throughout the entire plant–soil system. Specifically, the objectives of this study were (1) to understand the drought responsiveness of physicochemical soil properties in the rhizosheath, (2) to identify rhizosheath traits whose drought responses are controlled by intraspecific variability among crop varieties and (3) to establish mechanistic links between key plant trait modifications and rhizosheath soil drought effects in the context of holistic plant drought adaptation.

Materials and Methods

Soil and plant material

The soil material was collected from the ploughing horizon of a conventionally managed arable field (5–20 cm depth, 48°24′25″N 11°41′26″E). It was classified as Stagnic Luvisol (Humic, Loamic) (IUSS Working Group WRB, 2015). The excavated soil material was sieved to 2 mm, air-dried for 6 wk and homogenized by repeated mixing. Its basic physical and chemical properties are given in Table 1. The panel of 38 maize (*Zea*

Table 1 Properties of the sieved (< 2 mm) and air-dried soil material before the start of the experiment, including soil texture, mass distribution across aggregate size fractions (> 250, 250–53, < 53 µm), carbon (C) and nitrogen (N) concentrations.

Property	Soil material < 2 mm
pH	6.3
Sand (mg g^{-1} soil)	332
Silt (mg g^{-1} soil)	395
Clay (mg g^{-1} soil)	273
> 250 µm (mg g^{-1} soil)	790
250–53 µm (mg g^{-1} soil)	154
< 53 µm (mg g^{-1} soil)	56
C (mgC g^{-1} soil)	13.9
N (mgN g^{-1} soil)	1.4
C : N ratio	10.2
$\delta^{13}C$ (‰ VPDB)	−25.5

mays L.) varieties (16 landraces, 16 hybrids, 6 open-pollinated varieties; details in Supporting Information Table S1) was selected to cover the intraspecific plasticity of rhizosheath traits exhibited by central European crop varieties.

Experimental design and growth conditions

The pot experiment was conducted in a high-throughput phenotyping facility (48°24′25.7″N 11°43′23.2″E, LemnaTec Scanalyzer3D system; LemnaTec Gmbh, Aachen, Germany). The experiment was set up with two irrigation levels (well-watered and drought conditions) and 38 maize varieties, plus additional unplanted controls, resulting in a 2 × 39 full factorial design. The planted treatments were replicated four times and the control treatment three times with a total of 310 pots.

Rectangular boxes, hereafter referred to as mesocosms, served as pots (37 × 27 × 31 cm). The center of each mesocosm contained a Styrofoam block (20 × 25 × 27.5 cm) to avoid exceeding the weight limits of the facility, and the two resulting compartments were hydraulically connected by a thin soil layer underneath. Each mesocosm was filled with 9.9 kg of soil, and six maize seeds were sown in each pot and thinned to two plants after germination (one plant per mesocosm compartment each within 3.76 dm^3 of soil). The treatments were randomly arranged in the glasshouse and the pots were shuffled daily. Nutrients were added in three doses at rates of 450 mgN per plant and 70 mgS per plant as KNO_3, NH_4NO_3 and $MgSO_4{\cdot}7H_2O$. Initially, all pots were maintained under well-watered conditions by automatized daily watering to target weight. From Day 37 after sowing (DAS), half of the mesocosms remained at an average water potential of pF 1.7 (well-watered conditions), while the other half was exposed to soil drying by withholding irrigation (drought). Before the dry down, the soil surface was covered with plastic beads (PP copolymer) to reduce soil evaporation. The drying process was monitored gravimetrically by weighing the pots daily to calculate the normalized transpiration ratio (NTR) from the weight differences between consecutive days (for details, see Koehler *et al.*, 2023).

Root and soil sampling

The experiment was terminated at 64 DAS, when all plants under drought were stressed enough to reduce transpiration rates by at least 50% (NTR ≤ 0.5, Koehler *et al.*, 2023). The final water contents in well-watered and drought-stressed mesocosms at sampling were 22.7 ± 3.5 vol-% and 9.9 ± 1.5 vol-%, corresponding to pF values of 1.9 and pF 4.2. During the destructive sampling, we collected aboveground and belowground biomass and rhizosheath from all plants (Fig. S1). The root system of each plant was carefully excavated, and the rhizosheath was defined as the soil adhering to the root system after vigorous shaking on a vibration plate for 15 s. Coarse soil fragments (*c.* > 3 cm) that remained attached to the roots were carefully removed by hand. From each root system, an *c.* 20-cm fragment of a seminal root with the adhering rhizosheath was cut for soil enzyme assays. The rhizosheath of the entire remaining root system was carefully stripped by hand. In addition, broken roots in the non-rhizosheath soil were collected for 5 min, shaken manually, and the attached rhizosheath was sampled. For each plant, an aliquot of rhizosheath was air-dried for physicochemical analyses, and the total air-dried weight of rhizosheath was calculated from the total fresh weight times the water loss of the air-dried subsample. Gravimetric water contents at sampling were determined by drying 10 g of non-rhizosheath soil (105°C, 24 h). For the unplanted controls, aliquots of non-rhizosheath soil were collected and air-dried.

All roots collected during rhizosheath sampling were pooled, washed, and used to normalize specific rhizosheath mass by root biomass (g soil g^{-1} dry roots) or root length (g soil m^{-1} root). Additionally, a subsample of non-rhizosheath soil (500 g) from each plant was washed through a sieve to collect remaining roots, and to extrapolate quantitative root parameters such as root length, and root biomass to the root system of an entire plant by the weight ratio of the washed subsample to total soil. From each mesocosm, the root biomass of one plant was dried and weighed directly for chemical analyses, while the roots of the second plant were stored in 70% ethanol for root scanning, dried, and weighed afterwards.

Physicochemical soil analyses

Soil physicochemical analyses were performed on all rhizosheath samples, the unplanted controls, and the initial soil material. Soil samples from both compartments of the same mesocosm were pooled before analysis.

Aggregate size distribution was measured by dry sieving with a modified Casagrande device adapted from Felde *et al.* (2021). The soil material (maximum 3.00 ± 0.05 g) was placed on a sieve tower (250 and 53 µm), and each sample was subjected to a defined mechanical force by 2000 tapping cycles at a frequency of 180 cycles min^{-1}. Subsequently, three aggregate fractions were collected: macroaggregates (> 250 µm), large microaggregates (250–53 µm), and small microaggregates (< 53 µm), and their weight distribution was recorded. The two larger fractions were cleared of root litter by breaking large soil aggregates, removing

coarse root fragments with tweezers, and extracting small root residues by electrostatic attraction similar to Kaiser *et al.* (2009). In the fraction < 53 µm, no visible root debris was found. Subsequently, the fractions > 53 µm were ground in a ball mill.

Carbon, nitrogen (N) and ^{13}C contents were measured in all soil fractions using dry combustion with an isotope ratio mass spectrometer (Delta V Advantage; Thermo Fisher, Dreieich, Germany) coupled to an elemental analyzer (Euro EA, Eurovector, Milan, Italy, EA-IRMS). Results of ^{13}C measurements were determined as delta values ($\delta^{13}C$) relative to the Vienna Pee Dee Belemnite (V-PDB) standard.

Analyses of functional plant traits and soil enzymes

The dry matter content of biomass samples was calculated from its fresh weight and the water loss of subsamples dried at 40 and 105°C. Morphological root properties, such as root length, were assessed for all roots of one plant, after cutting them into fragments, scanning them on a flatbed scanner (600 DPI), and subsequent image analysis with RhizoVision Explorer v2.0.2 (broken roots analysis mode, image threshold level: 200, filter for non-root objects: maximum size of 0.5 mm^2, root pruning threshold during feature extraction: 5). Root tissue density (RTD) is expressed as root volume per biomass dry matter and specific root length (SRL) as the ratio of root length to biomass dry matter. Carbon, N, and ^{13}C contents of roots were measured by EA-IRMS in roots washed from the non-rhizosheath soil as $\delta^{13}C$ relative to V-PDB. The activity of soil enzymes involved in C, N, and phosphorus cycling (β-glucosidase, β-cellobiohydrolase, N-acetyl-glucosaminidase, acid phosphomonoesterase) was measured in the rhizosheath by assays with fluorescently labeled substrates (4-methylumbelliferyl β-D-glucopyranoside, 4-methylumbelliferyl β-D-cellobioside, 4-methylumbelliferyl N-acetyl-β--D-glucosaminide, 4-methylumbelliferyl phosphate; Dick *et al.*, 2018). The substrate release rate was determined as pmol h^{-1}.

Calculations

The proportion of plant-derived C ($\%C_{plant}$) in each aggregate fraction was calculated according to Balesdent & Balabane (1992):

$$\%C_{plant} = \frac{\left(\delta^{13}C_{RS} - \overline{\delta^{13}C_{BS}}\right)}{\left(\overline{\delta^{13}C_{R}} - \overline{\delta^{13}C_{BS}}\right)} \times 100$$

where $\delta^{13}C_{RS}$ is the $\delta^{13}C$ value of the aggregate fraction in the rhizosheath, $\overline{\delta^{13}C_{BS}}$ is the average $\delta^{13}C$ value of the same fraction in the unplanted controls, and $\overline{\delta^{13}C_{R}}$ is the $\delta^{13}C$ value in the root biomass averaged for the corresponding variety and irrigation treatment. $\%C_{plant}$ was set to zero in fractions depleted in ^{13}C compared to the unplanted controls.

To obtain plant-C concentrations (mgC g^{-1} fraction), $\%C_{plant}$ was multiplied by the C concentrations in the respective aggregate fractions. Element contents stored in each fraction (mg element g^{-1} soil) were calculated by multiplying the concentrations within the fraction (mg element g^{-1} fraction) by its mass proportion and summed to bulk element contents (mg element g^{-1} soil). Element contents in the rhizosheath per unit root length (mg element m^{-1} root) were calculated by multiplying bulk element contents with rhizosheath mass normalized to root length (g soil m^{-1} root). For each plant, total rhizosheath mass (g soil per plant) was calculated as the product of total root biomass (g roots per plant) and specific rhizosheath mass (g soil g^{-1} roots). Total rhizosheath mass was further multiplied by bulk plant-C contents to obtain total amounts of plant-C in the rhizosheath of one plant (mgC per plant). To avoid pseudoreplication, these parameters were averaged between both plants of one mesocosm.

Drought responsiveness (Δ Drought) of each soil and plant property was determined as the difference between the values of the drought-stressed samples and the average value of the well-watered samples of the same variety. As an indicator of drought tolerance, the relative loss of aboveground biomass (%Shoot reduction) under drought (DS) compared with the average under well-watered conditions (WW) was calculated as:

$$\%\text{Shoot reduction} = \frac{\left(\text{Shoot}_{DS} - \overline{\text{Shoot}_{ww}}\right)}{\overline{\text{Shoot}_{ww}}}$$

Subsequently, Δ Drought and shoot reduction were averaged within the same variety.

Statistical analyses

Statistical analyses were performed in R (v.4.0.4; R Core Team, 2021). Drought effects on physicochemical rhizosheath properties and the relevance of crop varieties in determining these drought responses were statistically tested with Bayesian Mixed Effects models (package BRMS; v.2.17.0; Bürkner, 2017, 2018, 2021). In each model, watering treatment was included as a fixed effect with well-watered conditions as reference factor level. Therefore, the slope of the linear models indicates the predicted change in the tested rhizosheath property from well-watered to drought-stressed conditions and is hereafter referred to as drought response. We considered drought responses as statistically significant if the 95% confidence interval (CI) of the slope did not overlap zero. For models with non-Gaussian response distributions, significance was assessed at the link scale. The drought effects presented in the text and figures are the predicted average changes in rhizosheath properties for all plants under drought conditions (mean and 95% CI). They were calculated from draws of the posterior predictive distribution as the difference between the two irrigation treatments. To test whether the individual varieties modified the drought response of rhizosheath properties, the models included a random slope and intercept for the different varieties. The random slope allows for assessing the divergence between the overall population drought response and the drought response of individual varieties. Variety effects were considered statistically significant if (1) the drought response of at least one variety differed from the drought response of the total population (95% CI of the random slope estimate did not

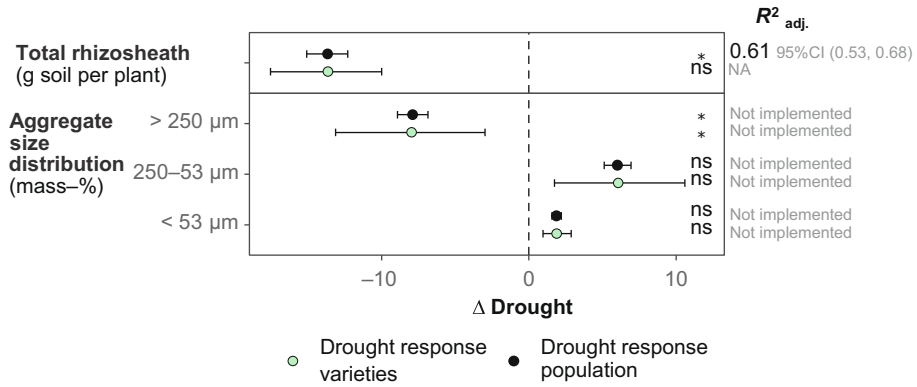

Fig. 1 Drought response (Δ Drought) in rhizosheath mass and aggregate size distribution. Displayed are the mean drought responses in the entire population of studied plants (black), and the range in the drought response of the corresponding rhizosheath property, taking the variability among maize varieties additionally into account (green). Drought effects are presented as the difference between well-watered and drought conditions in the unit of the response variable (mean and 95% confidence interval (CI) of the posterior predictions). A significant change in the rhizosheath property under drought is indicated by asterisks in the upper line. On the lower line, asterisks denote that individual varieties modified the drought response significantly, with one or more varieties exhibiting a significantly different drought response of the rhizosheath property compared to the entire population. Insignificance of drought effects (upper line) or variety effects (lower line) is indicated by ns. The adjusted R^2 values (mean and 95% CI) are reported for each model as marginal R^2 at the population level (upper line), which indicates the data variability explained solely by the watering treatment, and as conditional R^2 at the variety level (lower line), which represents the total data variability explained by the model including both watering treatment and variety effects. Conditional R^2 is not given (NA) in case of non-significant variety effects.

overlap zero), and (2) the overall standard deviation estimate of random variety slopes did not include zero as a lower boundary.

The magnitude of variety effects is presented in figures as posterior predictions (mean and 95% CI) for a new hypothetical variety whose group characteristics and variability are drawn from the total variability of all investigated varieties. A detailed description of model implementations and an overview of the computed models are given in Methods S1 and Table S2. For each model, the loo-adjusted marginal and conditional R^2 was calculated (package PERFORMANCE, v.0.9.0; Gelman *et al.*, 2019; Lüdecke *et al.*, 2021).

Furthermore, we conducted multiple regression analyses to explain variety-specific drought responses of rhizosheath properties with drought responses of functional plant traits. These regression analyses were performed for rhizosheath properties whose drought responses were previously found to be significantly modified among varieties. To select the relevant functional traits, an automated backward stepwise model reduction approach based on the Bayesian Information Criterion (BIC) was employed. Normal distribution of each response variable was confirmed by Shapiro–Wilk's test at $P < 0.05$. Multicollinearity among predictors was reduced by hierarchical variable clustering and selecting a representative predictor for highly clustered variables (Spearman's $\rho^2 > 0.3$, Fig. S2). Table S3 summarizes functional traits included as predictors in the model. All predictors were standardized, and the absence of redundancy between variables was confirmed by variance inflation factors below 5. Model residuals were checked using diagnostic plots. The drought response of rhizosheath properties and the drought responses of relevant functional traits were combined in a principal component analysis (PCA) using the prcomp function of the stats package. Correlation coefficients were calculated by Spearman's rank correlation and are denoted as ρ(df).

Results

Drought responsiveness of rhizosheath properties

Under drought stress, the total mass of rhizosheath adhering to the root system of one plant was significantly lower compared with well-watered conditions (Fig. 1), with drought-stressed plants having approximately four times less total rhizosheath mass (Table S4). The same trend was observed for rhizosheath normalized by root biomass (Fig. S3a) and root length (Fig. S3b). Rhizosheath mass normalized by root biomass correlated positively with the gravimetric water content at sampling under well-watered conditions ($\rho(150) = 0.48$, $P < 0.001$), whereas this was not observed under drought conditions ($\rho(149) = -0.05$, $P = 0.567$).

Under drought stress, aggregate stability in the rhizosheath was lower, as indicated by the significantly smaller mass contribution of the macroaggregate fraction (−7.9 mass-%, 95% CI (−8.9, −6.9); Fig. 1). This was related to the increased build-up of stable macroaggregates in well-watered samples compared with the initial soil material, while this was absent or less pronounced in dry rhizosheath samples ($> 250\,\mu m_{initial} = 79.0$ mass-%, $> 250\,\mu m_{-H_2O} = 80.4 \pm 4.2$ mass-%, $> 250\,\mu m_{+H_2O} = 88.3 \pm 3.2$ mass-%).

Bulk N (Fig. 2), SOC (Fig. S4), and plant-C concentrations (Fig. 2, +0.6 mgC g^{-1} soil, 95% CI (0.5, 0.7)) were significantly higher in the rhizosheath of drought-stressed plants compared with the rhizosheath of well-watered plants, while the bulk C : N ratio remained unaffected (Fig. 2). Conversely, element contents in the rhizosheath normalized to root length were lower under drought, which was significant for SOC and N (Fig. S3b, −0.4 mgN m^{-1} root, 95% CI (−0.5, −0.4)). Accordingly, drought stress led to a significant reduction in the total amount of plant-C remaining in the rhizosheath per plant (Fig. 2, −1.2

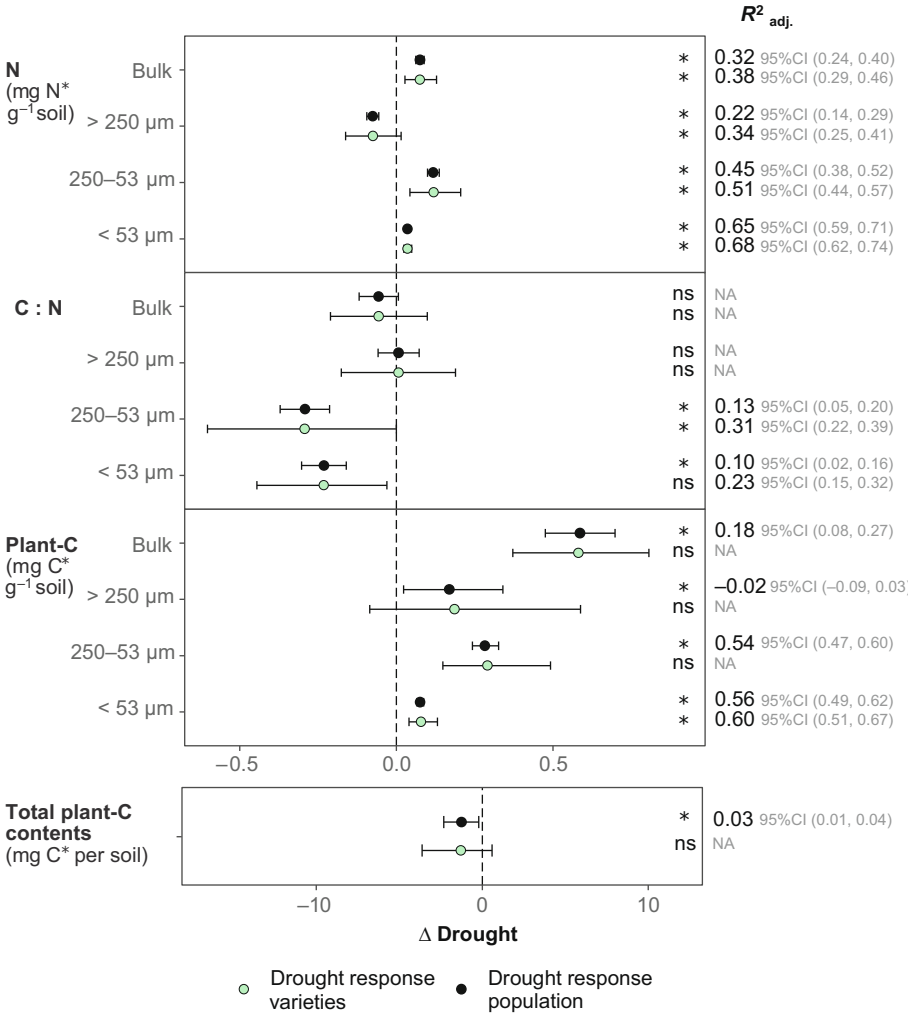

Fig. 2 Drought response of rhizosheath bulk nitrogen (N) and plant-carbon (plant-C) concentrations, element distribution across aggregate fractions, and total amounts of plant-C in the rhizosheath per plant. Displayed are the mean drought responses in the entire population of studied plants (black) and the range of drought responses of the corresponding rhizosheath property, taking the variability among maize varieties additionally into account (green). Drought effects (Δ Drought) are presented as the difference between well-watered and drought conditions in the unit of the response variable (mean and 95% confidence interval (CI) of the posterior predictions). A significant change in the rhizosheath property under drought is indicated by asterisks in the upper line. On the lower line, asterisks denote that individual varieties modified the drought response significantly, with one or more varieties exhibiting a significantly different drought response of the rhizosheath property compared to the entire population. Insignificance of drought effects (upper line) or variety effects (lower line) is indicated by ns. The adjusted R^2 values (mean and 95% CI) are reported for each model as marginal R^2 at the population level (upper line), which indicates the data variability explained solely by the watering treatment, and as conditional R^2 at the variety level (lower line), which represents the total data variability explained by the model including both watering treatment and variety effects. Conditional R^2 is not given (NA) in case of non-significant variety effects.

mgC per plant, 95% CI (−2.3, −0.2)), despite the low marginal R^2 (0.03, Fig. 2), suggesting that the difference in watering treatments poorly explains the variability in total plant-C.

On average, SOC, N, and plant-C were stored predominantly in the macroaggregate fraction under both watering treatments (Table 2). However, the distribution of plant-C contents across aggregate fractions varied widely among the rhizosheath samples of single plants, particularly in the macroaggregate fraction (Table 2). In general, plant-C contents in the macroaggregate fraction correlated positively with the soil C : N ratio in that fraction ($\rho(301) = 0.36$, $P < 0.001$), whereas plant-C contents in the microaggregates correlated negatively with the soil C : N ratio in the same fraction (250–53 µm: $\rho(301) = -0.39$, $P < 0.001$; < 53 µm: $\rho(301) = -0.32$, $P < 0.001$). Under drought, the distribution of SOC (Fig. S4), N (Fig. 2) and plant-C (Fig. 2) across aggregate fractions shifted, with increased element contents

Table 2 Aggregate-associated contents of soil organic carbon (SOC), nitrogen (N), and plant-carbon (plant-C) under well-watered (+H_2O) and drought-stressed conditions (−H_2O) averaged over the rhizosheath of all individual maize plants ± standard deviation.

	SOC (mgC g^{-1} soil)		N (mgN g^{-1} soil)		Plant-C (mgC g^{-1} soil)	
	+H_2O	−H_2O	+H_2O	−H_2O	+H_2O	−H_2O
> 250 µm	12.47 ± 0.69	11.71 ± 0.80	1.21 ± 0.06	1.14 ± 0.07	0.29 ± 0.41	0.43 ± 0.45
250–53 µm	1.57 ± 0.50	2.68 ± 0.66	0.15 ± 0.05	0.27 ± 0.07	0.08 ± 0.04	0.35 ± 0.17
< 53 µm	0.30 ± 0.07	0.63 ± 0.15	0.03 ± 0.01	0.07 ± 0.02	0.01 ± 0.01	0.09 ± 0.05

Table 3 Summary of minimal models explaining variety-specific drought responses of physicochemical rhizosheath properties based on drought responsiveness of functional traits.

	Drought response rhizosheath properties (dependent variables)						
	Δ > 250 μm	Δ N > 250 μm	Δ N 250–53 μm	Δ N < 53 μm	Δ Plant-C < 53 μm	Δ N bulk	Δ C : N 250–53 μm
Drought response plant traits and soil enzymes (predictors, $\beta^{Sig.\ level}$)							
Δ specific RS	1.64***	0.017*	−0.027***	–	–	−0.014*	0.12***
Δ grav. WC	–	−0.020*	–	–	−0.005*	−0.015**	–
Δ Root length	–	–	–	−0.003*	–	−0.009	0.10**
Δ RTD	−0.91	−0.035**	–	–	–	−0.019**	–
Δ R : S	–	–	–	–	–	−0.009	–
Δ C : N_{roots}	1.34**	0.025*	−0.013*	–	–	–	–
Δ N_{roots}	–	–	–	0.004**	0.007**	–	−0.07*
Δ Plant-C_{bulk}	−1.38**	−0.021*	0.018**	–	–	–	–
Δ Plant-C_{lmic}	–	–	–	0.006***	0.022***	0.013**	–
Δ CBH activity	–	–	–	–	–	0.009	−0.10**
Δ Pho activity	–	–	0.015*	–	–	–	–
Model performance							
Intercept	−7.91***	−0.074***	0.115***	0.035***	0.079***	0.076***	−0.29***
R^2 adjusted	0.42	0.31	0.51	0.5	0.75	0.51	0.47
BIC	255.92	−213.01	−238.17	−366.91	−315.67	−255.45	−121.29
F-value	$F_{4,33} = 7.65$***	$F_{5,32} = 4.29$**	$F_{4,33} = 10.6$***	$F_{3,34} = 13.42$***	$F_{3,34} = 38.07$***	$F_{7,30} = 6.47$***	$F_{4,33} = 9.33$***

Drought responses (Δ) are defined as the difference between drought samples and the average in well-watered controls within one maize variety. Each column represents one minimal model with the corresponding rhizosheath property as the response variable and the standardized regression coefficients of the functional traits ($\beta^{Sig.level}$, Significance levels: ***, $P < 0.001$; **, $P < 0.01$; *, $P < 0.05$) presented in the rows. These traits were selected as relevant predictors by model reduction. Blue font indicates a negative correlation between the drought responsiveness of the rhizosheath property and the drought response of the corresponding trait, while red indicates a positive correlation. *F*-values for each model are reported with their respective degrees of freedom and level of significance. Specific RS (specific rhizosheath; g soil g^{-1} root), grav.WC (gravimetric water content in the non-rhizosheath soil; mass-%), Root length (total root length per plant; m), RTD (root tissue density; g cm^{-3}), R : S (root : shoot ratio; g g^{-1}), C : N_{roots} (C : N root biomass; −), N_{roots} (nitrogen (N) concentration root biomass; mgN g^{-1} roots), Plant-C_{bulk} (bulk concentration of plant-carbon (plant-C); mgC g^{-1} soil), Plant-C_{lmic} (concentration of plant-C within fraction 250–53 μm; mgC g^{-1} fraction), CBH (cellobiohydrolase activity in the rhizosheath; pmol h^{-1}), PHO (phosphatase activity in the rhizosheath; pmol h^{-1}), > 250 μm (mass contribution of fraction > 250 μm; mass-%), N > 250, 250–53, > 53 μm (N content of corresponding fraction; mgN g^{-1} soil), plant-C < 53 μm (plant-C content of fraction < 53 μm; mgC g^{-1} soil), N bulk (bulk concentration of N; mgN g^{-1} soil), C : N 250–53 μm (C : N in fraction 250–53 μm; −), BIC (Bayesian Information Criterion).

observed in both microaggregate fractions. Particularly, the large microaggregates exhibited significantly increased contents of SOC (Fig. S4), N (Fig. 2) and plant-C (Fig. 2, +0.28 mgC g^{-1} soil; 95% CI (0.24, 0.33)) under drought. Simultaneously, the C : N ratio in both microaggregate fractions decreased significantly under drought (Fig. 2).

Variety effects on the drought responsiveness of rhizosheath properties

Variety effects on the reduction in total (Fig. 1) and normalized rhizosheath mass under drought (Fig. S3a,b) were negligible, as this was a universal trend for all varieties. While the lower weight share of macroaggregates in the dry rhizosheath was also a consistent trend among maize varieties, the magnitude of the drought-induced reduction in stable macroaggregates varied significantly among crop varieties (Fig. 1). The drought-induced reduction in the mass proportion > 250 μm ranged from -0.7 ± 3.5 mass-% macroaggregates to -15.0 ± 3.1 mass-% across variety averages (Table S4).

Variety effects were found to be of little importance in determining the drought response of bulk element concentrations in the rhizosheath, as only the magnitude of the drought-induced increase in bulk N concentrations varied significantly among maize varieties (Fig. 2).

However, variety effects had a significant impact on the magnitude of the drought-induced shift in element distributions across aggregate size classes. In particular, for N (Fig. 2) and SOC (Fig. S4), the magnitude of drought-induced changes in element contents within all fractions exhibited significant variation among varieties. In addition, variety effects had a significant impact on the drought-induced change in the C : N ratio in the fraction 250–53 μm (Fig. 2) and on the plant-C content in the fraction < 53 μm (Fig. 2).

Variety-specific trait modifications control drought responsiveness of rhizosheath properties

The variation in the drought responsiveness of rhizosheath properties between varieties can be partially explained by variety-specific modifications of certain plant traits and soil enzymes, as evidenced by the significant minimal regression models (Table 3). Specifically, the regression models revealed that varieties with elevated root N contents and enhanced net-rhizodeposition in the rhizosheath under drought promoted the strong enrichment of bulk N, the accumulation of C, N and plant-C in

New Phytologist

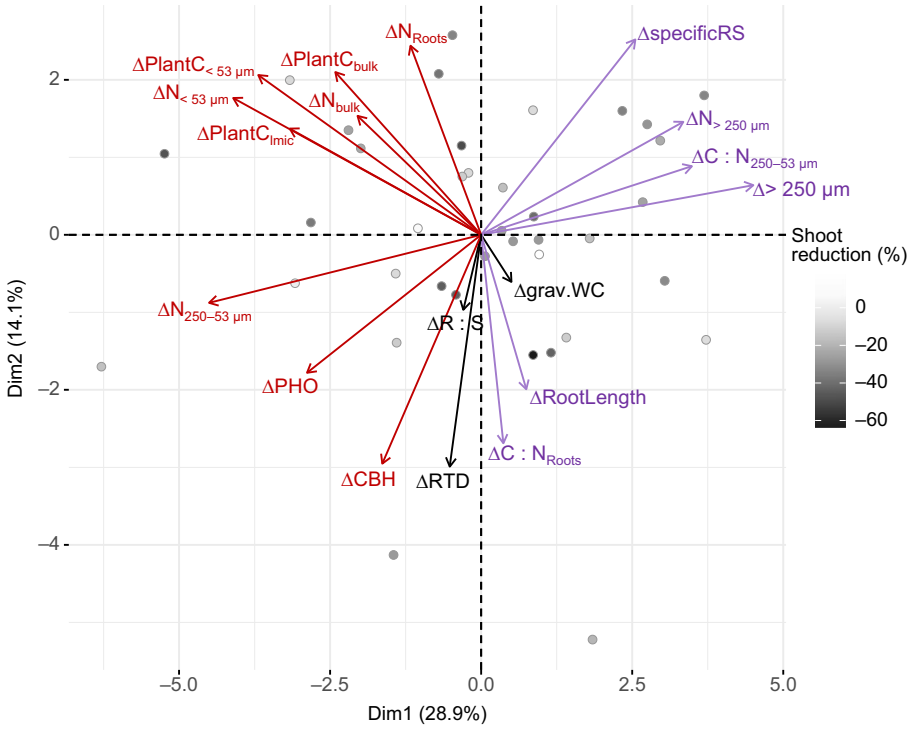

Fig. 3 The principal component analysis biplot displays the drought response (Δ) of rhizosheath properties, along with the drought response of plant traits and soil enzymes selected by model reduction. Plant and soil traits with arrows of the same color were positively associated with each other in the regression models (Table 3), while traits represented by black arrows were negatively associated with the drought response of all rhizosheath properties. Dots represent variety averages within the two-dimensional space, while the color gradient of their filling indicates the drought-induced reduction in aboveground biomass (Shoot reduction). The individual maize varieties can be identified in Supporting Information Fig. S5. SpecificRS (specific rhizosheath; g soil g^{-1} root), $N_{>\ 250\ \mu m}$ (nitrogen content of fraction > 250 µm; mgN g^{-1} soil), > 250 µm (mass contribution of fraction > 250 µm; mass-%), $C : N_{250–53\ \mu m}$ (C : N in fraction 250–53 µm; –), grav.WC (gravimetric water content in the non-rhizosheath soil; mass-%), RootLength (total root length per plant; m), $C : N_{roots}$ (C : N root biomass; –), R : S (root : shoot ratio; g g^{-1}), RTD (root tissue density; g cm^{-3}), CBH (cellobiohydrolase activity in the rhizosheath; pmol h^{-1}), PHO (phosphatase activity in the rhizosheath; pmol h^{-1}), $N_{250–53\ \mu m}$ (nitrogen content of fraction 250–53 µm; mgN g^{-1} soil), Plant-C_{lmic} (plant-carbon concentration within fraction 250–53 µm; mgC g^{-1} fraction), $N_{<\ 53\ \mu m}$ (nitrogen content of fraction <53 µm; mgN g^{-1} soil), Plant-$C_{<\ 53\ \mu m}$ (plant-carbon content of fraction <53 µm; mgC g^{-1} soil), Plant-C_{Bulk} (bulk concentration of plant-carbon; mgC g^{-1} soil), N_{Bulk} (bulk concentration of nitrogen; mgN g^{-1} soil), N_{roots} (nitrogen concentration of root biomass; mgN g^{-1} roots).

microaggregates, and a decrease of the soil C : N ratio in large microaggregates. Enhanced net rhizodeposition was indicated by increased bulk plant-C contents, and higher plant-C concentrations within the most enriched large microaggregate fraction (Tables 3, S5). Similarly, varieties with enhanced soil enzyme activities in the rhizosheath promoted greater accumulation of bulk N, C, and N in large microaggregates as well as decreasing soil C : N ratios in large microaggregates under drought (Tables 3, S5). By contrast, varieties that more strongly sustained rhizosheath mass under drought were found to better conserve macroaggregation and C and N contents in the macroaggregate fraction, while exhibiting stable or weakly increased soil C : N ratios in the large microaggregates (Tables 3, S5). Similarly, varieties that exhibited increased root elongation under drought maintained stable soil C : N ratios in the large microaggregates, while adversely affecting the accumulation of bulk N in the rhizosheath, as well as C and N in small microaggregates (Tables 3, S5). On the contrary, investment in costly roots, as indicated by higher root tissue density under drought, was consistently negatively associated with the drought response of assessed rhizosheath properties, as it caused lower preservation of macroaggregation, C and N contents in the large aggregate fraction, along with reduced accumulation of bulk N (Tables 3, S5).

Combining functional trait modifications selected by the regression models with rhizosheath drought responses in a PCA revealed a separation of opposing drought reactions of the plant–soil system along the first axis. All trait and rhizosheath responses that were positively associated with each other in the regression models were located either to the left or respectively to the right of the first axis (Fig. 3), with this gradient accounting for 28.9% of the observed variation in belowground drought reactions among varieties. Varieties more to the left of the first axis were under drought, characterized by a strong accumulation of C, N, and plant-C in the rhizosheath, particularly within microaggregates (Fig. 3; Table S3). Further, they were positively associated with preserved root N contents and greatly enhanced soil enzyme activities (phosphatase and cellobiohydrolase) within the rhizosheath under drought (Table 3; Fig. 3). Conversely, varieties further to the right of the first axis responded to drought by exhibiting increased element contents in the macroaggregate fraction,

enhanced preservation of rhizosheath mass and macroaggregation, along with higher or stable soil C : N ratios in microaggregates (Fig. 3; Table S3). This was associated with wider root C : N ratios and increased root elongation (Table 3; Fig. 3).

Plant drought tolerance, as indicated by the maintenance of vegetative biomass growth under drought, was not associated with distinct belowground drought reactions. Drought suppressed aboveground biomass formation in most varieties ($-24.36 \pm 16.69\%$), and the biomass decline scattered nondirectionally across the entire gradient of belowground drought reactions (Fig. 3).

Discussion

Soil moisture drives drought responses of rhizosheath mass and aggregate stability

We demonstrated an overall decrease in total and rhizosheath mass normalized to root length or root biomass under drought (Figs 1, S3a,b). This finding contradicts the common perception that plants promote rhizosheath formation in dry soils to cope with resource scarcity (Watt *et al.*, 1994; George *et al.*, 2014; Aslam *et al.*, 2022). However, these assumptions are primarily based on studies conducted with plants grown in sand-rich soils (Watt *et al.*, 1994; Haling *et al.*, 2013; Basirat *et al.*, 2019; Liu *et al.*, 2019), whereas finer textured soil material, as used in this study, has been shown to induce weaker rhizosheath formation (Bailey & Scholes, 1997; Brown *et al.*, 2017). Given the positive correlation between rhizosheath mass and soil water content at sampling under well-watered conditions, we posit that the higher soil moisture resulted in stronger physical soil adhesion to the root surface (Czarnes *et al.*, 1999). Consequently, the enhanced physical soil adhesion under wet conditions dominated over the potentially weakly enforced biological rhizosheath formation under dry conditions.

In line with rhizosheath formation, drought also altered rhizosheath soil structure by inhibiting the build-up of stable macroaggregates (Fig. 1). Since soil cohesion is stronger in wetter soils (Haines, 1925), this likely stabilized soil aggregates in the wet rhizosheath, and limits their disruption during excavation and subsequent air-drying. In addition, plant water uptake, transpiration, and daily rewatering in well-watered pots likely induced gentle wet-dry cycles in the rhizosheath, which can enhance aggregate tensile strength (Horn & Dexter, 1989; Materechera *et al.*, 1992). During each drying cycle, contracting water menisci pull soil particles together, increase interparticle contacts, and transport organic gluing substances toward contact points, subsequently stabilizing the formed soil aggregates (Horn & Dexter, 1989; Albalasmeh & Ghezzehei, 2014).

In summary, our study highlights that the drought response in rhizosheath formation and soil aggregation is primarily driven by soil moisture fluctuations, with higher soil moisture levels promoting increased structural stability. Thus, we encourage future research on plant–soil interactions to include soil hydrological properties for a more comprehensive interpretation of plant-driven processes.

Under drought, rhizodeposits in the rhizosheath accumulate in microaggregates through microbial processing

Drought stress caused higher concentrations of C, N, and plant-C in the rhizosheath, while the total amount of plant-derived C per plant was reduced (Figs 2, S4). These findings are consistent with previous studies reporting a reduction in total rhizodeposition in drought-exposed plants (Preece & Peñuelas, 2016; Holz *et al.*, 2018; Wang *et al.*, 2021), while the amount of C input per unit root length was preserved or increased on the expense of reduced root growth (Preece & Peñuelas, 2016; Holz *et al.*, 2018). Yet, the mechanisms driving the changes in net-rhizodeposition within the rhizosheath cannot be fully disentangled because it coincides with the altered rhizosheath volume under drought. Thus, the reduced total amount of plant-C within the rhizosheath under drought can be attributed either to a reduced input of plant-derived C or to the lower rhizosheath mass (Figs 1, 2). Accordingly, the higher concentrations of organic compounds in the drought-stressed rhizosheath can be the result of either a locally increased input or the spatial accumulation of root-derived compounds in the radially smaller rhizosheath. The latter is supported by the findings that rhizosheath mass, C, N, and plant-C contents are actually lower under drought when standardized to unit root length (Fig. S3b).

Drought stress had a significant impact on the distribution of organic compounds among aggregate size fractions, with higher C, N, and plant-C contents and lower soil C : N ratios in microaggregates compared with well-watered conditions (Figs 2, S4; Table 2). In general, soil C : N ratios in microaggregates decreased with increasing plant-C contents, whereas C : N ratios in macroaggregates conversely increased with higher plant-C contents. The distinct chemical composition of plant-derived compounds entering different aggregate fractions suggests different pathways of input. We hypothesize that macroaggregates received primarily particulate organic matter (POM) derived from root litter or root hairs, characterized by higher C : N ratios (e.g. C : N root biomass = 18.8). By contrast, microaggregates accumulated N-rich compounds such as rhizodeposits (e.g. maize exudates C : N = 5.1, Naveed *et al.*, 2017) or microbial compounds (e.g. soil microbial biomass C : N = 8.6, Cleveland & Liptzin, 2007). Drought stress facilitated the incorporation of N-rich compounds into microaggregates, suggesting a shift in the composition of retained rhizodeposits from well-watered to drought conditions. This shift likely involved a transition from heterogeneous root litter inputs predominantly stored in macroaggregates under well-watered conditions to the relative dominance of rhizodeposits directly retained or present as microbial-derived products, biomass or necromass in microaggregates. Given the higher activity of microbial-derived cellobiohydrolase in the rhizosheath of drought-stressed plants (Table S3; Blagodatskaya & Kuzyakov, 2008), we propose that the accumulation of N-rich compounds in the microaggregates occurred predominantly after the cycling of plant-derived C through the soil microbiome. Our hypothesis is visually supported by the high-resolution images of Vidal *et al.* (2018) and the work of Kaiser *et al.* (2015), revealing

that plant-derived C is primarily transferred to the soil microbiome rather than directly retained at the soil matrix.

Finally, the drought-induced shift in the composition of retained rhizodeposits by microbial processing explains why the increased plant-derived C content in the drought-stressed rhizosheath did not contribute to soil macroaggregation as described in previous studies (Morel *et al.*, 1991; Traore *et al.*, 2008; Baumert *et al.*, 2018). According to the aggregation mechanisms postulated by Tisdall & Oades (1982), Verchot *et al.* (2011), and Totsche *et al.* (2018), the incorporation of plant-C as microbial compounds reduces its effectiveness in stabilizing large-sized soil aggregates due to the size dependency between gluing agents and the resulting soil microstructure (Dorioz *et al.*, 1993).

In conclusion, our study demonstrated that drought stress reduced total rhizodeposition in the plant rhizosheath, while promoting its spatial accumulation in the rhizosheath and particularly within microaggregates through microbial processing. The enrichment of rhizodeposits as microbial products likely resulted in its reduced effectiveness for soil macroaggregation.

Variety-specific rhizosheath drought responses as intrinsic part of plant drought reaction

We demonstrated that the individual varieties significantly modified the drought responsiveness of several rhizosheath properties, such as the proportion of stable macroaggregates, bulk N content, C, N, and plant-C distribution across aggregate fractions, and soil C : N ratios within large microaggregates (Figs 1, 2, S4). The variable rhizosheath drought responsiveness among varieties was partially explained by the drought response of specific functional plant traits and soil enzymes (Table 3), highlighting that variety-specific prioritization of certain traits for soil resource acquisition can determine the drought responsiveness of rhizosheath traits.

The integration of rhizosheath properties, whose drought responses were modified by the different varieties, together with the drought response of root traits and soil enzymes, revealed a spectrum of opposing belowground strategies employed by the plant–soil system in response to drought stress (Table 3; Figs 3, 4). In the context of drought-inhibited photosynthesis (e.g. Ulrich *et al.*, 2022; Werner *et al.*, 2022), these divergent strategies were likely driven by different patterns of carbon partitioning throughout the plant–soil system. Accordingly, varieties associated with one end of the belowground strategy spectrum did not invest in increased net rhizodeposition or higher root construction costs under drought, as evidenced by the unchanged root tissue density and plant-C contents (Table 3; Fig. 3). This allowed them to direct more assimilated C toward root growth, indicated in their positive association with enhanced root elongation under drought (Lynch *et al.*, 2021; Table 3; Fig. 3). It can be argued that increased root elongation would enhance resource exploitation from a larger soil volume under field conditions (Lynch *et al.*, 2021). Furthermore, plant-derived compounds were retained in the rhizosheath of these varieties primarily as litter-derived POM, as supported by the stable or higher soil C : N ratios (Fig. 3). Particulate organic matter is known to be especially important in the formation of large aggregates (Bucka *et al.*, 2021). Thus, these varieties better preserved macroaggregation in the rhizosheath under drought (Fig. 3). Soil aggregation promotes the formation of finer intra-aggregate pores, which in turn enhance soil moisture retention (Cruz *et al.*, 2017) and water flow in dry soils (Carminati *et al.*, 2008), ultimately increasing plant-available water. The enhanced stabilization of rhizosheath mass under drought may further facilitate water and nutrient uptake in dry soils for these varieties (Fig. 3; Aslam *et al.*, 2022).

By contrast, varieties at the opposite end of the belowground strategy spectrum showed, as a reaction to drought, a strong accumulation of organic compounds within the rhizosheath at the expense of reduced root growth (Table 3; Fig. 3). We propose that the preservation of net-rhizodeposition in these varieties is a measure to buffer adverse effects on the soil microbiome and enzyme-mediated nutrient cycling. This hypothesis is supported by previous research demonstrating that higher mucilage concentrations and hotspots of root exudation stabilize exoenzyme activity and microbial biomass in dry soils (Ahmed *et al.*, 2018; Holz *et al.*, 2019; Zhang *et al.*, 2021). Accordingly, the accumulation of organic compounds in the rhizosheath of these varieties was positively related to greatly enhanced activities of cellobiohydrolase and acid phosphatase under drought (Table 3; Fig. 3). Cellobiohydrolases are produced by cellulose-degrading microorganisms, whereas phosphatases can be of microbial origin but are also produced by living roots (Blagodatskaya & Kuzyakov, 2008). Accordingly, the increased cellobiohydrolase activity was positively associated with decreasing soil C : N ratios and strong enrichment of microbially processed plant-derived and organic compounds within microaggregates in the rhizosheath of these varieties (Tables 3, S5; Fig. 3). Furthermore, preserved or enhanced root N levels as observed in these varieties have been demonstrated to be associated across species with qualitative root exudate compositions that are chemotactic to members of the soil microbiome (Williams *et al.*, 2022) and can induce increased soil respiration following drought (De Vries *et al.*, 2019). Thus, these varieties likely conserved nutrient cycling in the rhizosheath under drought, either by stabilizing the soil microbiome or by directly releasing enzymes for nutrient foraging. Moreover, the maintained microbial activity in the rhizosheath may alleviate plant drought stress through positive plant–microbial interactions, such as the production of phytohormones and the relief of oxidative stress (reviewed e.g. by Ahmad *et al.*, 2022; Naylor & Coleman-Derr, 2018).

In summary, our study identified divergent belowground strategies of the plant–soil system in response to drought by linking rhizosheath modifications and functional plant trait adaptations. Varieties ranged from those that prioritized soil exploration and sustained soil aggregation to those that invested assimilated C in enhanced net-rhizodeposition and sustained microbial interactions (Fig. 4). Thus, our study advocates for incorporating soil properties into a holistic understanding of belowground plant drought reaction. The incorporation of additional functional trait responses that influence both plant drought tolerance and physicochemical soil properties may help to explain the considerable variability in variety drought responses that is not captured by

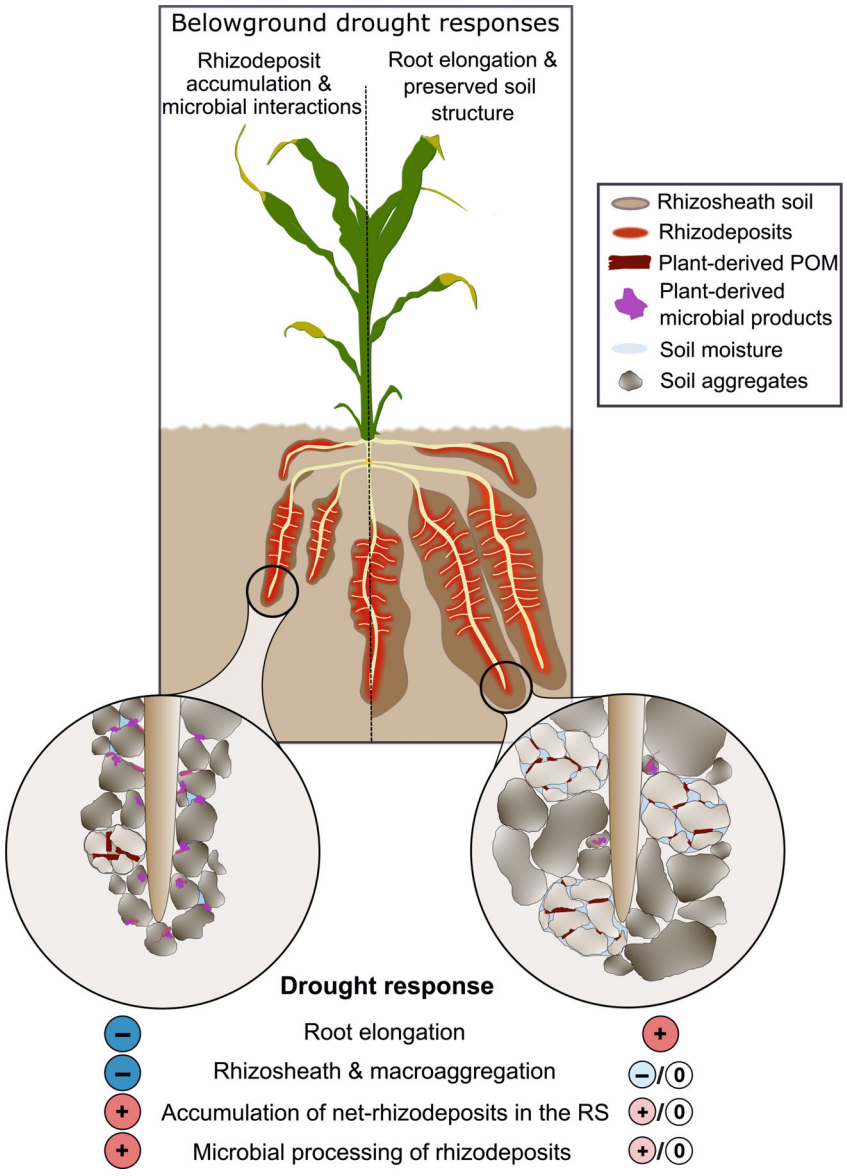

Fig. 4 Conceptual description of the opposing sides of the belowground strategy spectrum employed by the plant-rhizosheath system in response to drought. Maize varieties at one end of the spectrum respond to drought by strongly accumulating net-rhizodeposits in the rhizosheath (RS). This buffers drought effects on enzyme-mediated nutrient cycling and the soil microbiome, facilitates the enrichment of microbially processed rhizodeposits in microaggregates, and promotes the maintenance of beneficial plant–microbe interactions. By contrast, varieties at the other end of the spectrum respond to drought by increasing soil exploration through enhanced root elongation. In the rhizosheath of these varieties, rhizodeposits are retained primarily as particulate organic matter (POM), thus buffering the decrease in rhizosheath aggregation during soil desiccation. This leads to physical modifications of soil hydraulic properties in the root vicinity, likely promoting water retention in intra-aggregate pores and hydraulic connectivity within the larger rhizosheath.

the described strategy spectrum (Fig. 3). Promising traits to extend the concept include symbiosis with arbuscular mycorrhizal fungi, which enhance plant drought tolerance by influencing physiological drought response (Ren *et al.*, 2019) and by soil hydraulic modifications (Bitterlich *et al.*, 2018), or the presence of root hairs, which increase root water uptake (Carminati *et al.*, 2017) and promote rhizosheath formation (Brown *et al.*, 2017; Burak *et al.*, 2021). Although the belowground drought reactions did not translate into differences in plant drought tolerance in our experiment, it is crucial to test whether these strategies might promote yield resistance or plant survival under field conditions. We argue that, for example, the benefits of enhanced soil exploration through root elongation will be greater in the field than in a space-constrained pot experiment where root growth has likely reached saturation. Ultimately, considering holistic belowground drought reaction strategies may help to unlock the full potential of the plant–soil system for drought-resilient food production.

Conclusions

Drought stress substantially altered soil properties in the plant rhizosheath, proving the plastic response of these traits to drought. Overall, drought inhibited the formation of macroaggregates, while enhancing the accumulation of microbially processed rhizodeposits and organic compounds in microaggregates. Given the projected increase in drought frequency and severity, the cumulative effects of these small-scale changes at the root–soil interface may become vital for both plant drought tolerance and the drought resilience of soil organic carbon dynamics. The drought responsiveness of rhizosheath properties varied among varieties and is partly driven by variety-specific modifications of

functional plant traits and soil enzymes. This highlights the potential of targeting rhizosheath properties as phenotypic traits in trait-based research and crop breeding approaches. In conclusion, our study provides evidence that rhizosheath properties are an intrinsic phenotypic component of plant drought adaptation, similar to root morphology or physiology. The presented work provides first directions for incorporating rhizosheath properties into the framework of vegetative plant drought adaptation. We therefore advocate that future research on plant drought adaptation adopts a more holistic concept of the plant–soil system for climate-resilient crop production.

Acknowledgements

The work was funded by the German Bundesministerium für Bildung und Forschung within the collaborative project 'Rhizo4-Bio (Phase 1): RhizoTraits – Rhizosphären-Merkmale erhöhen die Resilienz der Erträge in modernen Anbausystemen, TP B' (funding no. 031B0908B). The authors thank Jorge Alberto Benitez Arevalo, Aniela Feldhofer, Bärbel Deischl, Michaela Henn and Christine Pfab for their great help with laboratory work and all people supporting us during long sampling hours in the greenhouse. Furthermore, we greatly acknowledge the support of the Statistical Consulting at TUM. Open Access funding enabled and organized by Projekt DEAL.

Competing interests

None declared.

Author contributions

FAS, AJW, NT, S-YT, TK, AC, JP, TL, SW, CWM and AV planned and designed the research. BE selected the investigated crop varieties and provided the seeds. FAS, AJW, NT, S-YT and TK established and maintained the experiment with support from WKV and JG. AJW, NT, S-YT and TK provided explanatory data on root morphology and root chemical composition, soil enzyme activities, plant biomass and monitoring of the soil drying experiment, respectively. FAS performed soil laboratory and data analyses with support of BDH. FB conducted elemental and isotopic soil measurements. FAS wrote the draft of the manuscript, with helpful input from AV and CWM. All authors contributed critically to the draft and gave final approval for publication.

ORCID

Franz Buegger https://orcid.org/0000-0003-3526-4711
Andrea Carminati https://orcid.org/0000-0001-7415-0480
Benjamin D. Hesse https://orcid.org/0000-0003-1113-9801
Tina Koehler https://orcid.org/0000-0002-6423-6835
Tillmann Lüders https://orcid.org/0000-0002-9361-5009
Carsten W. Mueller https://orcid.org/0000-0003-4119-0544
Johanna Pausch https://orcid.org/0000-0002-7102-4793
Franziska A. Steiner https://orcid.org/0009-0009-1152-1235
Shu-Yin Tung https://orcid.org/0000-0001-8892-6518
Nicolas Tyborski https://orcid.org/0009-0008-9031-3532
Alix Vidal https://orcid.org/0000-0002-5645-2730
Andreas J. Wild https://orcid.org/0000-0003-0754-461X
Sebastian Wolfrum https://orcid.org/0000-0003-0123-6720

Data availability

Soil data supporting the findings are available from the BonaRes Repository at Leibniz Centre for Agricultural Landscape Research (ZALF), Germany at doi: 10.20387/bonares-tdgx-339v. Root traits and biomass data will be linked to this dataset after an embargo no later than 12 months from the date of publication.

References

Adu MO, Asare PA, Yawson DO, Ackah FK, Amoah KK, Nyarko MA, Andoh DA. 2017. Quantifying variations in rhizosheath and root system phenotypes of landraces and improved varieties of juvenile maize. *Rhizosphere* **3**: 29–39.

Ahmad MH, Fiaz S, Hafeez S, Zahra S, Shah AN, Gul B, Aziz O, Rahman M-U, Fakhar A, Rafique M *et al.* 2022. Plant growth-promoting rhizobacteria eliminate the effect of drought stress in plants: a review. *Frontiers in Plant Science* **13**: 875774.

Ahmed MA, Sanaullah M, Blagodatskaya E, Mason-Jones K, Jawad H, Kuzyakov Y, Dippold MA. 2018. Soil microorganisms exhibit enzymatic and priming response to root mucilage under drought. *Soil Biology and Biochemistry* **116**: 410–418.

Alami Y, Achouak W, Marol C, Heulin T. 2000. Rhizosphere soil aggregation and plant growth promotion of sunflowers by an exopolysaccharide-producing *Rhizobium* sp. strain isolated from sunflower roots. *Applied and Environmental Microbiology* **66**: 3393–3398.

Albalasmeh AA, Ghezzehei TA. 2014. Interplay between soil drying and root exudation in rhizosheath development. *Plant and Soil* **374**: 739–751.

Angst G, Mueller KE, Nierop KG, Simpson MJ. 2021. Plant- or microbial-derived? A review on the molecular composition of stabilized soil organic matter. *Soil Biology and Biochemistry* **156**: 108–189.

Aslam MM, Karanja JK, Dodd IC, Waseem M, Weifeng X. 2022. Rhizosheath: An adaptive root trait to improve plant tolerance to phosphorus and water deficits? *Plant, Cell & Environment* **45**: 2861–2874.

Bailey C, Scholes M. 1997. Rhizosheath occurrence in South African grasses. *South African Journal of Botany* **63**: 484–490.

Bakhshandeh S, Corneo PE, Yin L, Dijkstra FA. 2018. Drought and heat stress reduce yield and alter carbon rhizodeposition of different wheat genotypes. *Journal of Agronomy and Crop Science* **205**: 157–167.

Balesdent J, Balabane M. 1992. Maize root-derived soil organic carbon estimated by natural ^{13}C abundance. *Soil Biology and Biochemistry* **24**: 97–101.

Basirat M, Mousavi SM, Abbaszadeh S, Ebrahimi M, Zarebanadkouki M. 2019. The rhizosheath: a potential root trait helping plants to tolerate drought stress. *Plant and Soil* **445**: 565–575.

Baumert VL, Vasilyeva NA, Vladimirov AA, Meier IC, Kögel-Knabner I, Mueller CW. 2018. Root exudates induce soil macroaggregation facilitated by fungi in subsoil. *Frontiers in Environmental Science* **6**: 140.

Bitterlich M, Sandmann M, Graefe J. 2018. Arbuscular mycorrhiza alleviates restrictions to substrate water flow and delays transpiration limitation to stronger drought in tomato. *Frontiers in Plant Science* **9**: 154.

Blagodatskaya E, Kuzyakov Y. 2008. Mechanisms of real and apparent priming effects and their dependence on soil microbial biomass and community structure: critical review. *Biology and Fertility of Soils* **45**: 115–131.

Blum A. 1996. Crop responses to drought and the interpretation of adaptation. *Plant Growth Regulation* **20**: 135–148.

Brown LK, George TS, Neugebauer K, White PJ. 2017. The rhizosheath – a potential trait for future agricultural sustainability occurs in orders throughout the angiosperms. *Plant and Soil* **418**: 115–128.

Bucka FB, Felde VJ, Peth S, Kögel-Knabner I. 2021. Disentangling the effects of OM quality and soil texture on microbially mediated structure formation in artificial model soils. *Geoderma* **403**: 115213.

Burak E, Quinton JN, Dodd IC. 2021. Root hairs are the most important root trait for rhizosheath formation of barley (*Hordeum vulgare*), maize (*Zea mays*) and *Lotus japonicus* (Gifu). *Annals of Botany* **128**: 45–57.

Bürkner P-C. 2017. BRMS: an R Package for bayesian multilevel models using STAN. *Journal of Statistical Software* **80**: 1–28.

Bürkner P-C. 2018. Advanced Bayesian multilevel modeling with the R Package BRMS. *The R Journal* **10**: 395–411.

Bürkner P-C. 2021. Bayesian item response modeling in R with BRMS and STAN. *Journal of Statistical Software* **100**: 1–54.

Carminati A, Kaestner A, Lehmann P, Flühler H. 2008. Unsaturated water flow across soil aggregate contacts. *Advances in Water Resources* **31**: 1221–1232.

Carminati A, Passioura J, Zarebanadkouki M, Ahmed MA, Ryan PR, Watt M, Delhaize E. 2017. Root hairs enable high transpiration rates in drying soils. *New Phytologist* **216**: 771–781.

Cheraghi M, Mousavi SM, Zarebanadkouki M. 2023. Functions of rhizosheath on facilitating the uptake of water and nutrients under drought stress: a review. *Plant and Soil* **491**: 1–25.

Cleveland CC, Liptzin D. 2007. C:N:P stoichiometry in soil: is there a "Redfield ratio" for the microbial biomass? *Biogeochemistry* **85**: 235–252.

Comas LH, Becker SR, Cruz VMV, Byrne PF, Dierig DA. 2013. Root traits contributing to plant productivity under drought. *Frontiers in Plant Science* **4**: 442.

Cruz BC, Furrer JM, Guo Y-S, Dougherty D, Hinestroza HF, Hernandez JS, Gage DJ, Cho YK, Shor LM. 2017. Pore-scale water dynamics during drying and the impacts of structure and surface wettability. *Water Resources Research* **53**: 5585–5600.

Czarnes S, Hiller S, Dexter A, Hallett P, Bartoli F. 1999. Root:soil adhesion in the maize rhizosphere: the rheological approach. *Plant and Soil* **211**: 69–86.

De La Fuente Cantó C, Simonin M, King E, Moulin L, Bennett MJ, Castrillo G, Laplaze L. 2020. An extended root phenotype: the rhizosphere, its formation and impacts on plant fitness. *The Plant Journal* **103**: 951–964.

De Vries FT, Brown C, Stevens CJ. 2016. Grassland species root response to drought: consequences for soil carbon and nitrogen availability. *Plant and Soil* **409**: 297–312.

De Vries FT, Williams A, Stringer F, Willcocks R, McEwing R, Langridge H, Straathof AL. 2019. Changes in root-exudate-induced respiration reveal a novel mechanism through which drought affects ecosystem carbon cycling. *New Phytologist* **224**: 132–145.

Dick RP, Dick LK, Deng S, Li X, Kandeler E, Poll C, Freeman C, Jones TG, Weintraub MN, Esseili KA *et al.* 2018. Cross-laboratory comparison of fluorimetric microplate and colorimetric bench-scale soil enzyme assays. *Soil Biology and Biochemistry* **121**: 240–248.

Dorioz JM, Robert M, Chenu C. 1993. The role of roots, fungi and bacteria on clay particle organization. An experimental approach. *Geoderma* **56**: 179–194.

Felde VJ, Schweizer SA, Biesgen D, Ulbrich A, Uteau D, Knief C, Graf-Rosenfellner M, Kögel-Knabner I, Peth S. 2021. Wet sieving vs dry crushing: soil microaggregates reveal different physical structure, bacterial diversity and organic matter composition in a clay gradient. *European Journal of Soil Science* **72**: 810–828.

Forsman A. 2015. Rethinking phenotypic plasticity and its consequences for individuals, populations and species. *Heredity* **115**: 276–284.

Gelman A, Goodrich B, Gabry J, Vehtari A. 2019. R-squared for Bayesian regression models. *The American Statistician* **73**: 307–309.

George TS, Brown LK, Ramsay L, White PJ, Newton AC, Bengough AG, Russell J, Thomas WTB. 2014. Understanding the genetic control and physiological traits associated with rhizosheath production by barley (*Hordeum vulgare*). *New Phytologist* **203**: 195–205.

Haines WB. 1925. Studies in the physical properties of soils: II. A note on the cohesion developed by capillary forces in an ideal soil. *The Journal of Agricultural Science* **15**: 529–535.

Haling RE, Brown LK, Bengough AG, Young IM, Hallett PD, White PJ, George TS. 2013. Root hairs improve root penetration, root-soil contact, and phosphorus acquisition in soils of different strength. *Journal of Experimental Botany* **64**: 3711–3721.

Holz M, Zarebanadkouki M, Carminati A, Hovind J, Kaestner A, Spohn M. 2019. Increased water retention in the rhizosphere allows for high phosphatase activity in drying soil. *Plant and Soil* **443**: 259–271.

Holz M, Zarebanadkouki M, Kaestner A, Kuzyakov Y, Carminati A. 2018. Rhizodeposition under drought is controlled by root growth rate and rhizosphere water content. *Plant and Soil* **423**: 429–442.

Horn RF, Dexter AR. 1989. Dynamics of soil aggregation in an irrigated desert loess. *Soil and Tillage Research* **13**: 253–266.

Intergovernmental Panel on Climate Change. 2023. Technical summary. In: *Climate change 2021: the physical science basis. Contribution of working group I to the sixth assessment report of the Intergovernmental Panel on Climate Change.* Cambridge, UK and New York, NY, USA: Cambridge University Press, 33–144.

IUSS Working Group WRB. 2015. *World Reference Base for Soil Resources 2014, update 2015. International soil classification system for naming soils and creating legends for soil maps.* Rome, Italy: FAO.

Jones DL, Nguyen C, Finlay RD. 2009. Carbon flow in the rhizosphere: carbon trading at the soil–root interface. *Plant and Soil* **321**: 5–33.

Kaiser C, Kilburn MR, Clode PL, Fuchslueger L, Koranda M, Cliff JB, Solaiman ZM, Murphy DV. 2015. Exploring the transfer of recent plant photosynthates to soil microbes: mycorrhizal pathway vs direct root exudation. *New Phytologist* **205**: 1537–1551.

Kaiser M, Ellerbrock RH, Sommer M. 2009. Separation of coarse organic particles from bulk surface soil samples by electrostatic attraction. *Soil Science Society of America Journal* **73**: 2118–2130.

Kallenbach CM, Frey SD, Grandy AS. 2016. Direct evidence for microbial-derived soil organic matter formation and its ecophysiological controls. *Nature Communications* **7**: 13630.

Karlowsky S, Augusti A, Ingrisch J, Akanda MKU, Bahn M, Gleixner G. 2018. Drought-induced accumulation of root exudates supports post-drought recovery of microbes in mountain grassland. *Frontiers in Plant Science* **9**: 1593.

Klein SP, Schneider HM, Perkins AC, Brown KM, Lynch JP. 2020. Multiple integrated root phenotypes are associated with improved drought tolerance. *Plant Physiology* **183**: 1011–1025.

Koehler T, Schaum C, Tung S-Y, Steiner F, Tyborski N, Wild AJ, Akale A, Pausch J, Lueders T, Wolfrum S *et al.* 2023. Above and belowground traits impacting transpiration decline during soil drying in 48 maize (*Zea mays* L.) genotypes. *Annals of Botany* **131**: 373–386.

Leng G, Hall J. 2019. Crop yield sensitivity of global major agricultural countries to droughts and the projected changes in the future. *The Science of the Total Environment* **654**: 811–821.

Liu T-Y, Ye N, Song T, Cao Y, Gao B, Zhang D, Zhu F, Chen M, Zhang Y, Xu W *et al.* 2019. Rhizosheath formation and involvement in foxtail millet (*Setaria italica*) root growth under drought stress. *Journal of Integrative Plant Biology* **61**: 449–462.

Lüdecke D, Ben-Shachar MS, Patil I, Waggoner P, Makowski D. 2021. PERFORMANCE: an R package for assessment, comparison and testing of statistical models. *Journal of Open Source Software* **6**: 3139.

Lynch JP, Strock CF, Schneider HM, Sidhu JS, Ajmera I, Galindo-Castañeda T, Klein SP, Hanlon MT. 2021. Root anatomy and soil resource capture. *Plant and Soil* **466**: 21–63.

Materechera SA, Dexter AR, Alston AM. 1992. Formation of aggregates by plant roots in homogenised soils. *Plant and Soil* **142**: 69–79.

Morel JL, Habib L, Plantureux S, Guckert A. 1991. Influence of maize root mucilage on soil aggregate stability. *Plant and Soil* **136**: 111–119.

Naveed M, Brown LK, Raffan AC, George TS, Bengough AG, Roose T, Sinclair I, Koebernick N, Cooper L, Hackett CA *et al.* 2017. Plant exudates may stabilize or weaken soil depending on species, origin and time. *European Journal of Soil Science* **68**: 806–816.

Naylor D, Coleman-Derr D. 2018. Drought stress and root-associated bacterial communities. *Frontiers in Plant Science* **8**: 2223.

Naylor D, Naasko K, Smith M, Couvillion S, Nicora C, Trejo J, Fransen S, Danczak R, McClure R, Hofmockel KS *et al.* 2023. Interactive effects of depth and differential irrigation on soil microbiome composition and functioning. *Frontiers in Microbiomes* **2**: 1078024.

Ndour PMS, Heulin T, Achouak W, Laplaze L, Cournac L. 2020. The rhizosheath: from desert plants adaptation to crop breeding. *Plant and Soil* **456**: 1–13.

North GB, Nobel PS. 1997. Drought-induced changes in soil contact and hydraulic conductivity for roots of *Opuntia ficus-indica* with and without rhizosheaths. *Plant and Soil* **191**: 249–258.

Palta JA, Gregory PJ. 1997. Drought affects the fluxes of carbon to roots and soil in ^{13}C pluse-labeled plants of wheat. *Soil Biology and Biochemistry* **29**: 1395–1403.

Pang J, Ryan MH, Siddique KHM, Simpson RJ. 2017. Unwrapping the rhizosheath. *Plant and Soil* **418**: 129–139.

Preece C, Peñuelas J. 2016. Rhizodeposition under drought and consequences for soil communities and ecosystem resilience. *Plant and Soil* **409**: 1–17.

R Core Team. 2021. *R: a language and environment for statistical computing.* Vienna, Austria: R Foundation for Statistical Computing.

Rabbi SM, Tighe MK, Warren CR, Zhou Y, Denton MD, Barbour MM, Young IM. 2021. High water availability in drought tolerant crops is driven by root engineering of the soil micro-habitat. *Geoderma* **383**: 114738.

Rabbi SM, Warren CR, Macdonald C, Trethowan RM, Young IM. 2022. Soil-root interaction in the rhizosheath regulates the water uptake of wheat. *Rhizosphere* **21**: 100462.

Ren A-T, Zhu Y, Chen Y-L, Ren H-X, Li J-Y, Abbott LK, Xiong Y-C. 2019. Arbuscular mycorrhizal fungus alters root-sourced signal (abscisic acid) for better drought acclimation in *Zea mays* L. seedlings. *Environmental and Experimental Botany* **167**: 103824.

Santini M, Noce S, Antonelli M, Caporaso L. 2022. Complex drought patterns robustly explain global yield loss for major crops. *Scientific Reports* **12**: 5792.

Schneider HM. 2022. Characterization, costs, cues and future perspectives of phenotypic plasticity. *Annals of Botany* **130**: 131–148.

Somasundaram S, Rao TP, Tatsumi J, Iijima M. 2009. Rhizodeposition of mucilage, root border cells, carbon and water under combined soil physical stresses in *Zea mays* L. *Plant Production Science* **12**: 443–448.

Spinoni J, Vogt JV, Naumann G, Barbosa P, Dosio A. 2018. Will drought events become more frequent and severe in Europe? *International Journal of Climatology* **38**: 1718–1736.

Tisdall JM, Oades JM. 1982. Organic matter and water-stable aggregates in soils. *Journal of Soil Science* **33**: 141–163.

Totsche KU, Amelung W, Gerzabek MH, Guggenberger G, Klumpp E, Knief C, Lehndorff E, Mikutta R, Peth S, Prechtel A *et al.* 2018. Microaggregates in soils. *Journal of Plant Nutrition and Soil Science* **181**: 104–136.

Traore O, Groleau-Renaud V, Plantureux S, Tubeileh A, Boeuf-Tremblay V. 2008. Effect of root mucilage and modelled root exudates on soil structure. *European Journal of Soil Science* **51**: 575–581.

Ulrich DEM, Clendinen CS, Alongi F, Mueller RC, Chu RK, Toyoda J, Gallegos-Graves LV, Goemann HM, Peyton B, Sevanto S *et al.* 2022. Root exudate composition reflects drought severity gradient in blue grama (*Bouteloua gracilis*). *Scientific Reports* **12**: 12581.

Verchot LV, Dutaur L, Shepherd KD, Albrecht A. 2011. Organic matter stabilization in soil aggregates: understanding the biogeochemical mechanisms that determine the fate of carbon inputs in soils. *Geoderma* **161**: 182–193.

Vidal A, Hirte J, Bender SF, Mayer J, Gattinger A, Höschen C, Schädler S, Iqbal TM, Mueller CW. 2018. Linking 3D soil structure and plant-microbe-soil carbon transfer in the rhizosphere. *Frontiers in Environmental Science* **6**. doi: 10.3389/fenvs.2018.00009.

Wang R, Cavagnaro TR, Jiang Y, Keitel C, Dijkstra FA. 2021. Carbon allocation to the rhizosphere is affected by drought and nitrogen addition. *Journal of Ecology* **109**: 3699–3709.

Watt M, McCully ME, Canny MJ. 1994. Formation and stabilization of rhizosheaths of *Zea mays*. Effect of soil water content. *Plant Physiology* **106**: 179–186.

Werner LM, Hartwig RP, Engel I, Franzisky BL, Wienkoop S, Brenner M, Preiner J, Repper D, Hartung J, Zörb C *et al.* 2022. Local and systemic metabolic adjustments to drought in maize: hydraulic redistribution in a split-root system. *Journal of Plant Nutrition and Soil Science* **185**: 632–642.

Williams A, Langridge H, Straathof AL, Muhamadali H, Hollywood KA, Goodrace R, De Vries FT. 2022. Root functional traits explain root exudation rate and composition across a range of grassland species. *Journal of Ecology* **110**: 21–33.

Zhang X, Bilyera N, Fan L, Duddel P, Ahmed MA, Carminati A, Kaestner A, Dippold MA, Spielvogel S, Razavi BS. 2023. The spatial distribution of rhizosphere microbial activities under drought: water availability is more important than root-hair-controlled exudation. *New Phytologist* **237**: 780–792.

Zhang X, Myrold DD, Shi L, Kuzyakov Y, Dai H, Hoang DTT, Dippold MA, Meng X, Song X, Li Z *et al.* 2021. Resistance of microbial community and its functional sensitivity in the rhizosphere hotspots to drought. *Soil Biology and Biochemistry* **161**: 108360.

Supporting Information

Additional Supporting Information may be found online in the Supporting Information section at the end of the article.

Fig. S1 Images of the mesocosms and the destructive root and soil sampling.

Fig. S2 Hierarchical variable clustering to test for multicollinearity among multiple regression predictors.

Fig. S3 Drought response of normalized rhizosheath mass and bulk element concentrations normalized to root length.

Fig. S4 Drought response of rhizosheath bulk C concentrations and C distribution across aggregate fractions.

Fig. S5 Principal components analysis biplot of the drought response of rhizosheath properties, plant functional traits, and soil enzymes, additionally identifying the individual varieties.

Methods S1 Bayesian Mixed Effects model implementation with BRMS.

Table S1 Summary of the studied maize varieties and their characteristics.

Table S2 Detailed description of the computed Mixed Effects models for each rhizosheath property.

Table S3 Summary of drought responses of functional traits considered as multiple regression predictors.

Table S4 Average soil properties of the initial soil material before incubation and the rhizosheath of each maize variety under both irrigation treatments.

Table S5 Summary of the minimal model explaining variety-specific drought responses of soil organic carbon distribution based on drought responsiveness of functional traits.

Please note: Wiley is not responsible for the content or functionality of any Supporting Information supplied by the authors. Any queries (other than missing material) should be directed to the *New Phytologist* Central Office.